

# A Capacitive Loading Method for Turning a Single-Band Antenna Into Dual-Band for Wireless Terminal Applications

Jiangwei Sui , Student Member, IEEE, and Ke-Li Wu , Fellow, IEEE

**Abstract**—This letter proposes a simple method to turn a single-band inverted-F antenna (IFA) or loop antenna into a dual-band antenna with a small frequency ratio and similar radiation patterns by simply adding a capacitor near the shorting end of a conventional single-band IFA or a loop antenna. Two demonstration examples imitating a mobile terminal application using IFA and loop antenna are present. The measured results show that the IFA and loop antenna with an added capacitor near the shorting end have comparable radiation patterns and total efficiencies in the two designed frequency bands compared with the antennas without the capacitor. The measured frequency ratio of the two resonances is 1.15 (2.23 and 2.56 GHz) for IFA and 1.19 (2.19 and 2.61 GHz) for loop antenna. And the two resonant frequencies can be easily controlled by tuning the added capacitor so that this method can be easily applied to frequency agility applications. To illustrate the physical mechanism, a transmission line model is presented and analyzed.

**Index Terms**—Capacitive load, dual-band, frequency agility, IFA, loop antenna, radiation pattern, small frequency ratio.

## I. INTRODUCTION

TO MEET the needs of higher data rate and ubiquitous connection, dual-band antenna has been widely used in mobile terminals due to the space, weight, and cost constraints. Among various dual-band antennas, the dual-band antennas with small frequency ratio are desired in many applications, such as carrier aggregation (CA) (2.2 and 2.7 GHz, ratio as 1.23) [1], satellite communication (21 and 26 GHz, ratio as 1.24) [2], radio frequency identification (842.5 and 922.5 MHz, ratio as 1.1) [3], and global positioning system scenarios (1.227 and 1.575 GHz, ratio as 1.28) [4].

Among various internal antennas for mobile terminals, inverted-F antenna (IFA) is one of the most popular antennas due to its low profile, high design flexibility, and compactness [5]. For dual-band IFA, the most straightforward method is using different radiating arms to generate multiple resonances [6]. Parasitic elements can also be used to generate an additional

resonance [7]. Another method to realize a dual-band IFA is to introduce an LC resonator on the radiating patch of the antenna [8]. A twisted line can also be used to achieve a dual-band IFA [9]. Modifying the ground plane is another effective technique to achieve a dual-band antenna [10], [11].

Besides IFAs, loop antennas have also been widely used in mobile terminals in the form of metal frame antennas on smart phones [12], [13]. A dual-band loop antenna can be achieved by utilizing the multimode characteristic of a loop itself [14]–[17]. However, the frequency ratio of these multiple modes is usually large so that it will be inapplicable for some applications requiring small frequency ratio.

Incorporating lumped elements into antennas to tune the resonance and impedance matching is widely used. Adding a capacitive load at the open end [18] or radiating arm [1] of the planar IFA can effectively decrease the resonant frequency of the antenna. In [19], a series resonator containing lumped elements is added to the open end of an IFA to achieve two resonances at 2.45 and 5.8 GHz with a large frequency ratio of 2.36. In [20], two stubs, each with a varactor diode, are incorporated to the short end and open end of an IFA to control the first two resonant frequencies and the frequency ratio is around 2. In [21], a shunt capacitor is added in parallel to the feed conductor to solve the impedance mismatch problem at the high frequency and the frequency ratio of the two resonances is as large as 2.24 (2.45 and 5.5 GHz).

In this letter, a simple but effective method is proposed for turning a conventional single-band IFA or loop antenna into a dual-band antenna with a small frequency ratio and similar radiation patterns by adding a capacitor near the shorting end of the antenna. Compared with prior works that use lumped capacitors, the most attractive feature of the proposed method is that it can generate a new resonance in addition to the original resonance and these two resonances have a small frequency ratio and similar radiation patterns. Although there is also a varactor on the short end of the IFA in [20], it is only used to tune the high resonant frequency. However, in our work, the capacitor is used to generate a low resonant frequency apart from the high resonant frequency. And this is why we can achieve two resonances with a small frequency ratio (around 1.15), whereas the frequency ratio is around 2 in [20].

The content of this letter is organized as follows: Section II introduces a demonstration example of the proposed method on IFA and presents a transmission line model to analyze the physical mechanism. Section III presents an implementation of the proposed method on loop antennas. Finally, a conclusion is given in Section IV.

Manuscript received August 29, 2018; revised October 13, 2018; accepted October 25, 2018. Date of publication October 29, 2018; date of current version November 29, 2018. This work was supported by Postgraduate Scholarship of The Chinese University of Hong Kong. (Corresponding author: Ke-Li Wu.)

The authors are with the Department of Electronic Engineering, The Chinese University of Hong Kong, Hong Kong (e-mail: jwsui@ee.cuhk.edu.hk; kluwu@cuhk.edu.hk).

Digital Object Identifier 10.1109/LAWP.2018.2878614

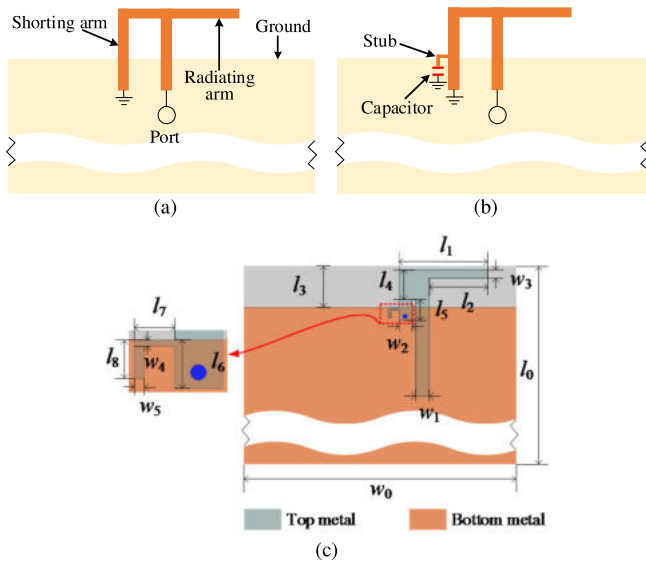


Fig. 1. Configurations of IFAs. (a) Conventional IFA. (b) IFA with a capacitor. (c) Dimensions. The shorting pin is indicated by a blue dot.

TABLE I  
DIMENSIONS OF PROPOSED IFA (UNIT: MM)

$l_0$	100	$l_3$	10	$l_6$	3	$w_0$	65	$w_3$	2
$l_1$	21	$l_4$	7	$l_7$	2.5	$w_1$	3.1	$w_4$	0.4
$l_2$	14	$l_5$	5	$l_8$	2.4	$w_2$	3	$w_5$	0.6

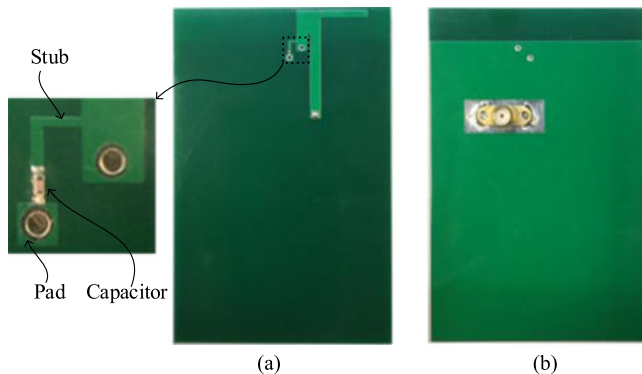


Fig. 2. Prototype of the dual-band IFA with a capacitor. (a) Top view. (b) Bottom view.

## II. DUAL-BAND IFA

### A. Antenna Configuration

As shown in Fig. 1(a), a conventional IFA consists of a feeding port, a shorting arm and a radiating arm. According to the proposed method, as shown in Fig. 1(b), a grounding capacitor is added on the shorting arm at a proper position near the shorting end. For comparison purpose, a conventional IFA and its counterpart with a capacitor are designed and measured. The dimensions of the capacitor loaded IFA are marked in Fig. 1(c) with specific values given in Table I. The substrate for the PCB board is FR4 with thickness of 1.6 mm and relative permittivity of 4.3. Fig. 2 shows the prototype of the capacitor loaded

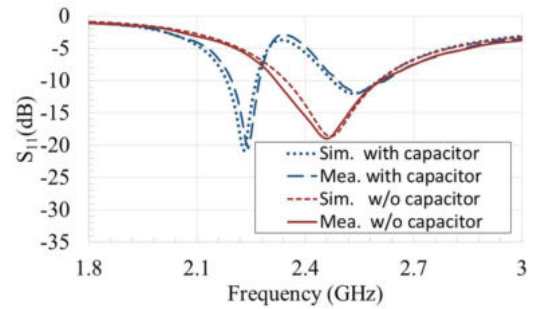


Fig. 3. The matching of the IFAs with and without the capacitor.

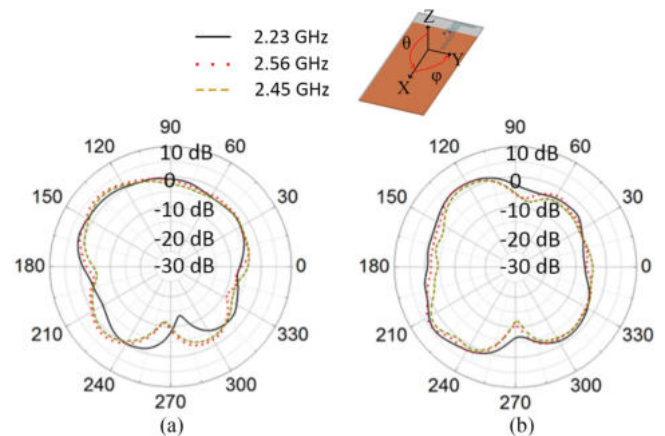


Fig. 4. Measured radiation patterns for the IFA with the capacitor at 2.23 and 2.56 GHz and the IFA without capacitor at 2.45 GHz. (a)  $x$ - $o$ - $y$  plane. (b)  $x$ - $o$ - $z$  plane.

IFA and a zoom-in view of the soldered capacitor is shown in Fig. 2(a).

As presented in Fig. 3, the conventional IFA without the capacitor exhibits a single resonance at 2.45 GHz. By adding a 0.9 pF capacitor at the shorting arm, two resonances at 2.23 GHz and 2.56 GHz are generated. The measured results agree well with the simulated results.

The radiation performance for the IFAs with and without the capacitor is also measured using the in-house SATIMO SG128 spherical near-field scanner in an ISO17025 accredited laboratory. The measured gain patterns for the IFA with the capacitor at 2.23 GHz and 2.56 GHz and that of the conventional IFA at 2.45 GHz are compared in Fig. 4. It is seen that the antennas have similar radiation patterns at these frequencies in both the  $x$ - $o$ - $y$  plane and the  $x$ - $o$ - $z$  plane. The measured total efficiencies and simulated radiation efficiency are presented in Fig. 5, showing that the IFA with the capacitor achieves comparable total efficiency in both bands compared to that of the conventional IFA in its working band.

To understand the dual-resonance mechanism, the simulated surface current distributions of the conventional IFA working at 2.45 GHz and the dual-band IFA at 2.23 and 2.56 GHz are plotted in Fig. 6. The difference of the current distribution near the capacitor results in different equivalent length of the shorting arm at 2.23 and 2.56 GHz that determines the resonant frequencies, whereas the similar radiation characteristics mainly rely on the current distribution on the radiating arm of the IFA, which are nearly the same. This also explains why there exist

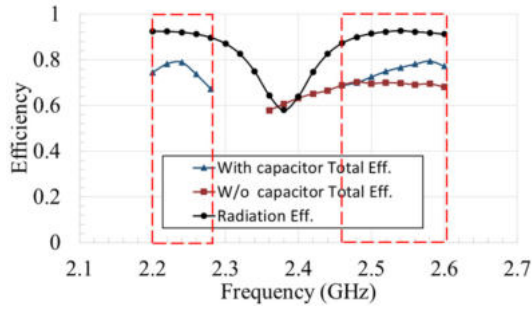


Fig. 5. Measured total efficiency and simulated radiation efficiency for the IFAs.

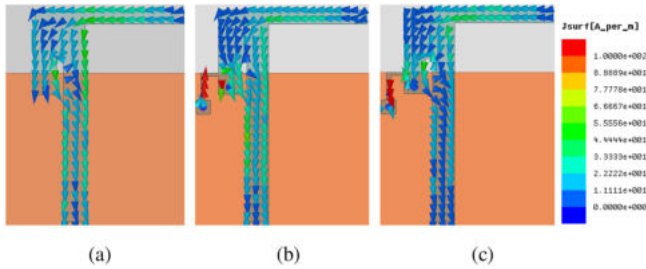


Fig. 6. Simulated current distributions. (a) Conventional IFA at 2.45 GHz. (b) Capacitor loaded IFA at 2.23 GHz. (c) Capacitor loaded IFA at 2.56 GHz.

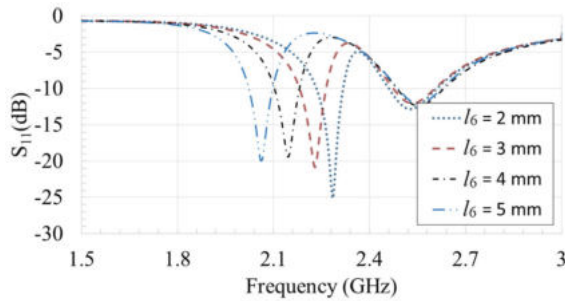


Fig. 7. Simulated  $S_{11}$  of the IFA for different tapping positions with a 0.9 pF capacitor.

two resonances in our antenna and the structure in [20] only controls the high resonance. The position of the tapping point of the capacitor is parametrically studied in Fig. 7. It can be seen that with the same 0.9 pF capacitor, different tapping position  $l_6$  will lead to different frequency ratio of the two resonances.

### B. Transmission Line Model

To explain the dual-resonance mechanism, a simple transmission line model is presented. As shown in Fig. 8(a), a conventional IFA can be modeled as a shorted quarter wavelength transmission line with an open end [1], [8]. It should be noted that this model only concerns with the resonant frequency of the antenna but not the input impedance at the feeding port as the radiation resistance is not involved. It is known that for a typical IFA, the antenna resonates when the sum of the admittances looking toward both sides of an observation point,  $Y_{short}$  and  $Y_{open}$ , is zero. The corresponding transmission line model for the IFA with a capacitor is shown in Fig. 8(b), where the

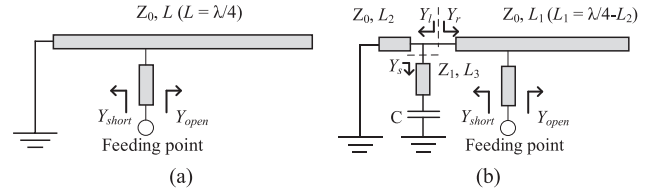


Fig. 8. Transmission line models. (a) Conventional IFA. (b) Proposed dual-band IFA.

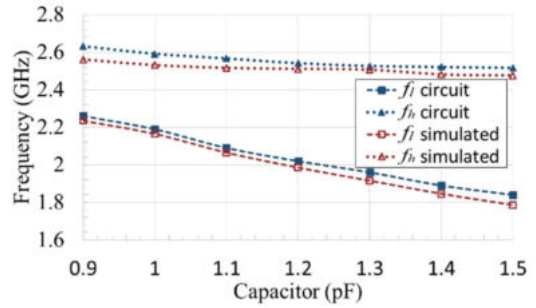


Fig. 9. Comparison of the two resonant frequencies versus capacitance obtained from the circuit model and the EM simulated result.  $Z_1$  is estimated for 0.4 mm width,  $Z_0$  for 3 mm width,  $L_3$  as 9 mm, and  $L_2$  as 3.1 mm.

observation point is chosen at the tapping position. The physical structures seen toward the shorting end and the open end are modeled by the transmission lines of  $(Z_0, L_2)$  and  $(Z_0, \lambda/4 - L_2)$ , respectively. Here,  $\lambda$  is the wavelength at the resonant frequency of the conventional IFA without a capacitor. The short high impedance stub is added on the shorting arm of the IFA and is modeled by a short transmission line  $(Z_1, L_3)$ . Assume  $Y_s$ ,  $Y_r$ , and  $Y_l$  are the input admittances seen toward the capacitor, the open end and the shorting end, respectively. At the observation point, the resonance occurs when

$$Y_l + Y_r = 0 \quad (1)$$

where

$$Y_l = -j \frac{1}{Z_0} \cot(\beta L_2) + Y_s \quad (2)$$

$$Y_r = j \frac{1}{Z_0} \tan(\beta L_1) \quad (3)$$

and

$$Y_s = j \frac{1}{Z_1} \frac{Z_1 + \frac{1}{\omega C} \tan(\beta L_3)}{\frac{1}{\omega C} - Z_1 \tan(\beta L_3)}. \quad (4)$$

Here,  $\beta$  is the propagation constant and  $\omega$  is the angular frequency. It can be found from this model that the generation of the two resonances lies in the fact that the admittance  $Y_s$  is negative at  $f_h$  and positive at  $f_l$ . This difference will lead to the desired admittances of  $Y_l$  at the two resonances  $f_l$  and  $f_h$ , which contributes to the final generation of two resonances with small frequency ratio. This admittance difference coincides well with the difference of current direction on the capacitive load at  $f_l$  and  $f_h$  as shown in Fig. 6. The two resonant frequencies ( $f_l$  and  $f_h$ ) versus the capacitance obtained from the transmission line model and the EM simulated results are compared in Fig. 9, which coincide well with each other.

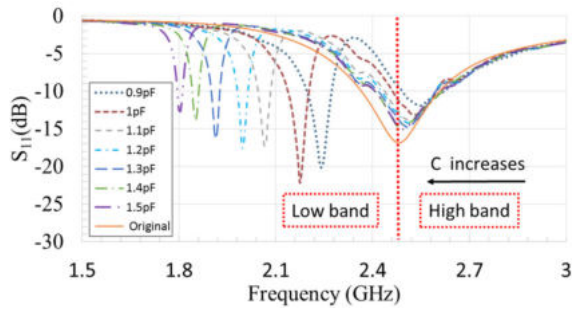


Fig. 10. Measured  $S_{11}$  of the IFA versus capacitor values.

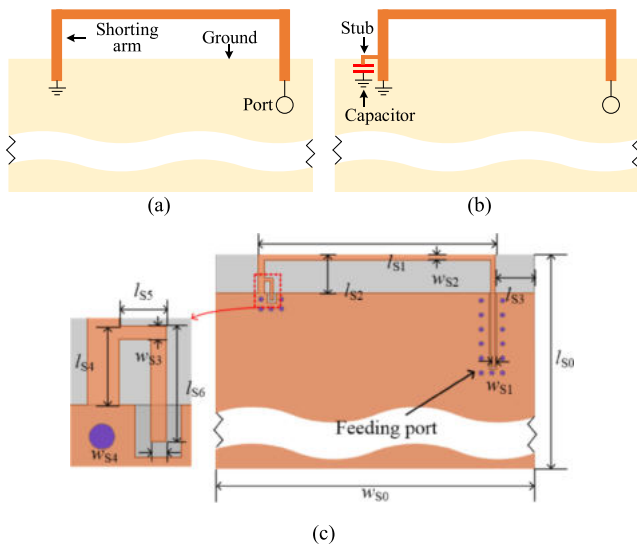


Fig. 11. Configurations of the loop antennas. (a) Conventional loop antenna. (b) Loop antenna with a capacitor. (c) Dimensions.

The effect of capacitor value is studied in Fig. 10. It can be seen that both the high and low resonances decrease when the capacitor value increases. However, the high resonance frequency is always higher than the resonant frequency of the original IFA, while the low resonant frequency can be easily tuned far apart from that of the conventional IFA. In this case, the high resonant frequency works at LTE band 41, whereas the low resonant frequency can be easily tuned to many other LTE bands, such as bands 1, 2, 3, and 4, which is quite attractive for the CA application. Another important observation is that the working frequency can be lowered from 2.45 to 1.8 GHz, which is equivalent to a size reduction about 26.5%.

### III. DUAL-BAND LOOP ANTENNA

The concept of adding a capacitor near the shorting end can also be applied to a loop antenna for dual-band applications.

The configurations of the loop antennas without and with the capacitor are shown in Fig. 11 and the substrate used for the prototype is FR4 with thickness of 0.8 mm. The dimensions for the dual-band loop antenna are marked in Fig. 11(c) and the detailed values are listed in Table II.

As shown in Fig. 12(a), the conventional loop antenna exhibits a single resonance at 2.35 GHz. By adding a 0.9 pF capacitor near the shorting end, two resonances at 2.19 and 2.61 GHz

TABLE II  
DIMENSIONS OF PROPOSED LOOP ANTENNAS (UNIT: MM)

$l_{S0}$	100	$l_{S3}$	8	$l_{S6}$	4.4	$w_{S2}$	1.2
$l_{S1}$	48.2	$l_{S4}$	3	$w_{S0}$	65	$w_{S3}$	0.5
$l_{S2}$	8	$l_{S5}$	1.8	$w_{S1}$	1	$w_{S4}$	0.6

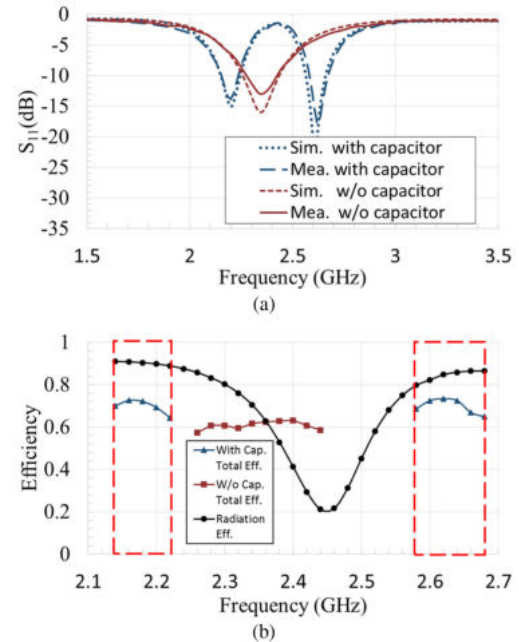


Fig. 12. Matching and efficiencies of the loop antennas. (a) Matching. (b) Measured total efficiency and simulated radiation efficiency.

(frequency ratio as 1.19) can be obtained. The total efficiency and radiation efficiency plotted in Fig. 12(b) shows that the loop antenna with the capacitor can achieve a similar efficiency at 2.19 and 2.61 GHz with that of the conventional loop antenna without a capacitor at 2.35 GHz.

One limitation should be discussed is that the bandwidths of the two resonances depend on the bandwidth of the original single resonance, as can be seen from Figs. 3 and 12(a). Another observation is that the ground clearances in the two designs are a little large regarding the trend of current full view display for smart phones. In fact, this capacitive loading method is also applicable to an antenna with small ground clearance as long as it is an IFA or loop antenna, which can be verified from the transmission line model shown in Fig. 8.

### IV. CONCLUSION

In this letter, a simple but effective method is proposed for turning a conventional single-band IFA or loop antenna into a dual-band antenna with a small frequency ratio and similar radiation patterns by adding a capacitor near the shorting end. Two demonstration examples for IFA and loop antenna are designed and measured. The results show that an IFA or a loop antenna with a capacitor exhibits a similar radiation efficiency and patterns in the dual designed frequency bands as those of the single-band antenna. The attractive features of this method such as simplicity and compactness make it a promising solution for the dual-band antennas with a small frequency ratio in smart phones and other mobile terminals.

## REFERENCES

- [1] B. Avser and G. M. Rebeiz, "Tunable dual-band antennas for 0.7–1.1 GHz and 1.7–2.3 GHz carrier aggregation systems," *IEEE Trans. Antennas Propag.*, vol. 63, no. 4, pp. 1498–1504, Apr. 2015.
- [2] W. Li, K. D. Xu, X. Tang, Y. Yang, Y. Liu, and Q. H. Liu, "Substrate integrated waveguide cavity-backed slot array antenna using high-order radiation modes for dual-band applications in K-band," *IEEE Trans. Antennas Propag.*, vol. 65, no. 9, pp. 4556–4565, Sep. 2017.
- [3] Z. Wang, R. She, J. Han, S. Fang, and Y. Liu, "Dual-band dual-sense circularly polarized stacked patch antenna with a small frequency ratio for UHF RFID reader applications," *IEEE Access*, vol. 5, pp. 15260–15270, 2017.
- [4] M.-S. Wang, X.-Q. Zhu, Y.-X. Guo, and W. Wu, "Miniaturized dual-band circularly polarized quadruple inverted-F antenna for GPS applications," *IEEE Antennas Wireless Propag. Lett.*, vol. 17, no. 6, pp. 1109–1113, Jun. 2018.
- [5] Z. Ying, "Antennas in cellular phones for mobile communications," *Proc. IEEE*, vol. 100, no. 7, pp. 2286–2296, Jul. 2012.
- [6] Z. D. Liu, P. S. Hall, and D. Wake, "Dual-frequency planar inverted-F antenna," *IEEE Trans. Antennas Propag.*, vol. 45, no. 10, pp. 1451–1458, Oct. 1997.
- [7] J. Anguera, I. Sanz, J. Mumburu, and C. Puente, "Multiband handset antenna with a parallel excitation of PIFA and slot radiators," *IEEE Trans. Antennas Propag.*, vol. 58, no. 2, pp. 348–356, Feb. 2010.
- [8] G. K. H. Lui and R. D. Murch, "Compact dual-frequency PIFA designs using LC resonators," *IEEE Trans. Antennas Propag.*, vol. 49, no. 7, pp. 1016–1019, Jul. 2001.
- [9] J.-H. Kim, W.-W. Cho, and W.-S. Park, "A small dual-band Inverted-F antenna with a twisted line," *IEEE Antennas Wireless Propag. Lett.*, vol. 8, pp. 307–310, 2009.
- [10] Z. Bao, Y. X. Guo, and R. Mittra, "Single-layer dual-/tri-band inverted-F antennas for conformal capsule type of applications," *IEEE Trans. Antennas Propag.*, vol. 65, no. 12, pp. 7257–7265, Dec. 2017.
- [11] Y. Cho and H. Yoo, "Miniaturised dual-band implantable antenna for wireless biotelemetry," *Electron. Lett.*, vol. 52, no. 12, pp. 1005–1007, 2016.
- [12] H. Chen and A. P. Zhao, "LTE antenna design for mobile phone with metal frame," *IEEE Antennas Wireless Propag. Lett.*, vol. 15, pp. 1462–1465, 2016.
- [13] Y.-L. Ban, Y.-F. Qiang, Z. Chen, K. Kang, and J.-H. Guo, "A dual-loop antenna design for hepta-band WWAN/LTE metal-rimmed smartphone applications," *IEEE Trans. Antennas Propag.*, vol. 63, no. 1, pp. 48–58, Jan. 2015.
- [14] K. L. Wong and C. H. Huang, "Printed loop antenna with a perpendicular feed for penta-band mobile phone application," *IEEE Trans. Antennas Propag.*, vol. 56, no. 7, pp. 2138–2141, Jul. 2008.
- [15] K. Ishimiya, C. Y. Chiu, and J. I. Takada, "Multiband loop handset antenna with less ground clearance," *IEEE Antennas Wireless Propag. Lett.*, vol. 12, pp. 1444–1447, 2013.
- [16] D. Wu, S. W. Cheung, and T. I. Yuk, "A compact and low-profile loop antenna with multiband operation for ultra-thin smartphones," *IEEE Trans. Antennas Propag.*, vol. 63, no. 6, pp. 2745–2750, Jun. 2015.
- [17] H. Xu *et al.*, "A compact and low profile loop antenna with six resonant modes for LTE smartphone," *IEEE Trans. Antennas Propag.*, vol. 64, no. 9, pp. 3743–3751, Sep. 2016.
- [18] C. R. Rowell and R. D. Murch, "A compact PIFA suitable for dual frequency 900/1800 MHz operation," *IEEE Trans. Antennas Propag.*, vol. 46, no. 4, pp. 596–598, Apr. 1998.
- [19] J. H. Kim and C.-H. Ahn, "Small dual-band inverted F antenna using series resonator," *Microw. Opt. Technol. Lett.*, vol. 59, no. 7, pp. 1489–1493, Jul. 2017.
- [20] M.-J. Lee, Y.-S. Kim, and Y. Sung, "Frequency reconfigurable planar inverted-F antenna (PIFA) for cell-phone applications," *Prog. Electromagn. Res.*, vol. 32, pp. 27–41, 2012.
- [21] Y. Liu *et al.*, "Miniaturization of dual band PIFA for wireless LAN communication," *ETRI J.*, vol. 35, no. 3, pp. 530–533, 2013.